Equatorial zonal plasma drifts measured by the C/NOFS satellite during the 2008–2011 solar minimum

Bela G. Fejer,[1] Brian D. Tracy,[1] and Robert F. Pfaff[2]

Received 8 February 2013; revised 31 May 2013; accepted 3 June 2013; published 26 June 2013.

[1] We use the measurements by the Vector Electric Field Investigation (VEFI) on board the Communication/Navigation Outage Forecasting System (C/NOFS) satellite to study the local time and seasonal- and longitudinal-dependent climatology of equatorial *F* region zonal plasma drifts during 2008–2011. These drifts are essentially westward during the day and eastward at night. Over Jicamarca Radio Observatory, the satellite measurements are in good agreement with incoherent scatter radar drifts. Our data show strong longitudinal variations, particularly in the South American sector during the solstices. The equinoctial data exhibit short-lived and largely enhanced westward drifts near sunrise and wave-4 structures from the early afternoon to late night equinoctial periods. The nighttime eastward drifts are largest near the western American sector at all seasons. The June solstice postmidnight eastward drifts decrease sharply at longitudes of about 310° and have much smaller values in the entire Eastern Hemisphere. We also briefly discuss the relationship between the longitude-dependent vertical and zonal plasma drifts.

Citation: Fejer, B. G., B. D. Tracy, and R. F. Pfaff (2013), Equatorial zonal plasma drifts measured by the C/NOFS satellite during the 2008–2011 solar minimum, *J. Geophys. Res. Space Physics*, *118*, 3891–3897, doi:10.1002/jgra.50382.

1. Introduction

[2] Quiet-time ionospheric electrodynamic ($\mathbf{E} \times \mathbf{B}$) plasma drifts are driven mostly by the dynamo effects of thermospheric winds and lower atmospheric waves [e.g., *Richmond*, 1995; *Heelis*, 2004; *Maute et al*., 2012]. Most past studies of low-latitude ionospheric electrodynamics have focused on the morphology and effects of meridional/cross field (vertical at the equator) plasma drifts. However, ionospheric zonal plasma drifts also play important roles on nighttime low-latitude *F* region plasma densities [e.g., *Pavlov*, 2006], on the shift of wave-4 structure in low-latitude total electron content [*Wan et al*., 2008], and on the generation and development of large-scale equatorial plasma irregularities (plasma depletions) [e.g., *Su et al*., 2009]. In addition, the daily variation of the zonal plasma drifts determines the degree of decoupling between the local and universal time experienced by magnetic flux tubes [*Murphy and Heelis*, 1986].

[3] Equatorial *F* region zonal plasma drifts have been studied extensively at the Jicamarca Radio Observatory (11.9°N, 76.8°W, magnetic dip 2°N) using incoherent scatter radar measurements. These drifts are westward during the day with typical values of about 40 m/s, which are largely independent of season and solar flux [e.g., *Fejer*, 1997, 2011]. The nighttime drifts are eastward, with peak values during the premidnight sector that increase from about 90 to 180 m/s from solar minimum to maximum. The postmidnight eastward drifts decrease with local time and reverse direction to westward near dawn [e.g., *Fejer et al*., 1991]. Enhanced geomagnetic activity drives perturbation zonal drifts which are largest at night and during equinox and December solstice [e.g., *Fejer et al*., 2005]. Spaced receiver scintillation measurements [e.g., *Valladares et al*., 1996; *Sheehan and Valladares*, 2004] showed that the zonal drifts of large-scale nighttime *F* region plasma irregularities (plasma bubbles) are in good agreement with radar-measured ambient drifts, except in the early night sector (typically before 2200 LT), when the rapid height rise of these irregularities leads to large decorrelations of the receiver signals [e.g., *Bhattacharyya et al*., 2001]. Recently, airglow imaging techniques were also used to study the zonal drifts of large-scale equatorial plasma irregularities and their relationship to the thermospheric zonal wind [e.g., *Sobral et al*., 2009, 2011; *Chapagain et al*., 2011, 2012].

[4] *Coley and Heelis* [1989] and *Coley et al*. [1994] used ion drift meter (IDM) measurements on board the polar orbiting Dynamics Explorer 2 (DE-2) satellite during the August 1981 to February 1983 high solar flux period to study the local-time dependence of longitudinally averaged middle- and low-latitude *F* region zonal drifts, their relationship to thermospheric winds, and response to geomagnetic activity. *Maynard et al*. [1995] showed that equatorial zonal drifts derived from electric field measurements on board the San Marco satellite were consistent with previous results. *Jensen and Fejer* [2007] examined the longitudinal dependence of the DE-2 zonal drifts but only in large local time

[1]Center for Atmospheric and Space Sciences, Utah State University, Logan, Utah, USA.
[2]NASA Goddard Space Flight Center, Greenbelt, Maryland, USA.

Corresponding author: B. G. Fejer, Center for Atmospheric and Space Sciences, Utah State University, 4405 Old Main Hill, Logan, UT 84322–4405, USA. (bela.fejer@usu.edu)

2169-9380/13/10.1002/jgra.50382

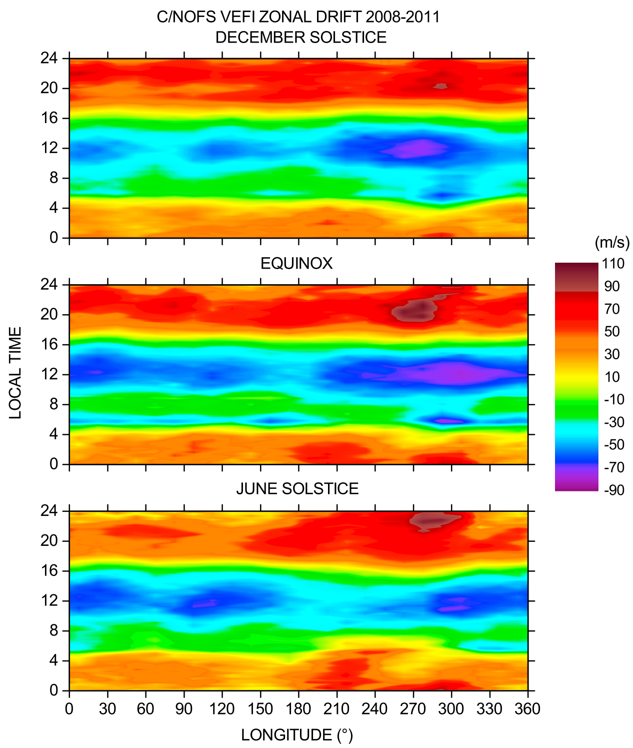

Figure 1. Seasonal and longitudinal dependence of the quiet-time equatorial average zonal drifts (positive eastward) measured on board the C/NOFS satellite.

bins and selected seasons since local time and seasonal coverage were locked together in these measurements. *Huang et al.* [2010] presented equatorial zonal drifts and ion densities measured on board the Defense Meteorological Satellites Program (DMSP) F13 and F14 satellites near dusk at geocentric altitudes of about 850 km showing wave number-4, number-3, and number-2 patterns during equinox, northern summer, and northern winter, respectively, and anticorrelated June and December solstice zonal drifts in regions of large magnetic declinations. *Pfaff et al.* [2010] presented initial *F* region zonal drifts derived from the Vector Electric Field Investigation (VEFI) measurements on board the Communication/Navigation Outage Forecasting System (C/NOFS) satellite and their longitudinal dependence, but for the limited time of 9 May to 4 July 2008. *Pacheco et al.* [2011] studied middle- and low-latitude quiet zonal drifts during the 1999–2003 high solar flux period using IDM and retarding potential analyzer data from Republic of China Satellite-1 (ROCSAT-1). They reported that within 15° of the magnetic equator, the nighttime average eastward drifts are larger (smaller) than daytime westward drifts during December solstice and equinox (June solstice). Very recently, *Huang et al.* [2012] studied ion-neutral coupling in the equatorial ionosphere during the 2008–2010 deep solar minimum using plasma density and drift measurements from C/NOFS and neutral densities and tides determined from Gravity Recovery and Climate Experiment (GRACE) satellite. Their nightside data show wave-4 tidal structuring and colocated extended regions of large plasma density decreases, strong downward drifts, and minima in zonal drifts with climatology similar to that of DE-3 nonmigrating tides [e.g., *Hagan and Forbes*, 2002, 2003].

[5] In this work, we study the local time, seasonal, and longitudinal dependence of equatorial *F* region zonal plasma drifts measured on board C/NOFS during the very low solar minimum of 2008–2011. Our data indicate that in the Eastern Hemisphere the longitudinal dependence of these drifts is largely season independent. In the Western Hemisphere, however, the longitudinal dependence changes considerably with season, as a result of magnetic declination and thermospheric wind effects. The C/NOFS zonal drifts in the American sector are consistent with incoherent scatter radar-measured drifts and nighttime thermospheric winds. We also briefly discuss the relationship between the longitudinal variations of equatorial zonal and vertical plasma drifts.

2. Measurements and Data

[6] The C/NOFS satellite was launched on 17 April 2008 into a 401 × 867 km orbit with a 13° inclination and an orbital period of 97.3 min. This mission was designed to improve the understanding and forecasting of equatorial scintillations [*de la Beaujardiere et al.*, 2004]. The satellite has various instruments that measure thermospheric plasma and neutral parameters. These include the Vector Electric Field Investigation (VEFI), which gathers electric and magnetic field measurements, and the Planar Langmuir Probe that provides plasma density and temperatures. The main VEFI instrument is a three-axis double probe electric field detector which includes three orthogonal 20 m tip-to-tip probes. Ionospheric electric fields (**E** × **B** plasma drifts) in geomagnetic coordinates are derived from the VEFI data by the subtraction of the corotation electric field (**V**scx**B**) and baseline offsets. The estimated accuracy of the 1 s DC electric field data used in our study is about 0.3–0.5 mV/m, which corresponds to a drift velocity of about 12–20 m/s. Additional characteristics and capabilities of these probes and the data processing techniques are described by *Pfaff et al.* [2010].

[7] The C/NOFS measurements are unevenly distributed in altitude and magnetic latitude as a result of the elliptical low-inclination (13°) satellite orbit. These measurements are most frequent near perigee and apogee and also close to the satellite's highest northern and southern latitudes. Since the geographic latitude of the geomagnetic equator changes by about 20° as a function of longitude, the satellite measurements cover a relatively large longitude-dependent range of geomagnetic latitudes and apex heights.

[8] We used 10 s averages of the 1 s quiet-time ($Kp \leq 3$) VEFI zonal plasma drifts measured during the May 2008 to February 2011 very low solar flux (average F10.7 index of about 80) period. Since the equatorial zonal drifts vary with magnetic latitude [e.g., *Pacheco et al.*, 2011], we have restricted our database to measurements within 5° of the dip equator. We deleted average drifts with standard deviations larger than 10 m/s to minimize nighttime ionospheric irregularity effects and with magnitudes larger than 200 m/s. The average apex altitude of our daytime climatological drifts is about 650 km; the nighttime drifts correspond to somewhat higher average altitudes in longitudinal sectors with high plasma irregularity occurrence [e.g., *Dao et al.*, 2011].

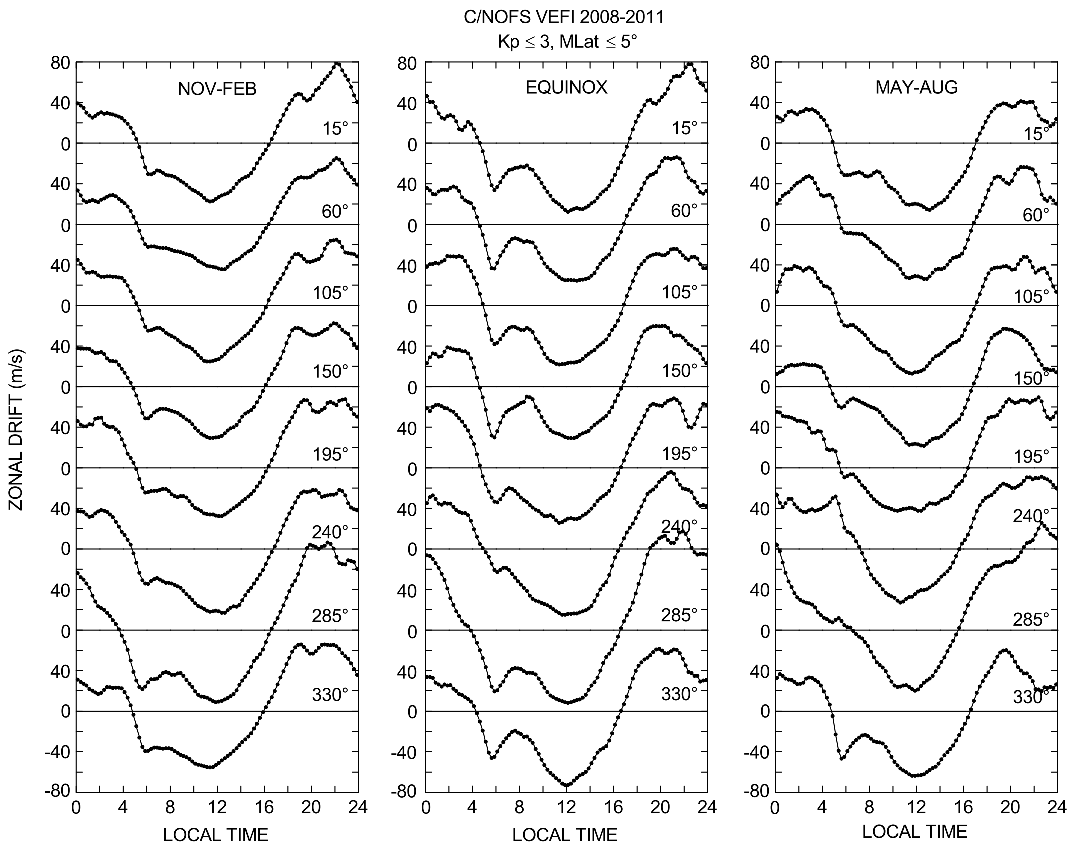

Figure 2. Local time and seasonal dependence of equatorial average zonal drifts (positive eastward) in eight longitudinal sectors.

3. Results and Discussion

[9] In this section, we present our initial results on the morphology of equatorial zonal drifts measured by C/NOFS focusing on their season- and longitude-dependent climatology and compare them with results from previous studies using ground-based and satellite observations.

3.1. General Results

[10] We determined the climatology of the quiet-time ($Kp \leq 3$) equatorial zonal plasma drifts by averaging the C/NOFS VEFI measurements within 5°of the magnetic equator in 15 min local time and 15° longitudinal bins. Figure 1 shows the local time and longitude dependence of these drifts for equinox (March–April and September–October), June solstice (May–August), and December solstice (November–February). Figure 1 shows westward drifts during the day and eastward at night. The early morning equinoctial data show strongly enhanced short-lived westward velocity peaks over almost the entire longitudinal range. The midday and early afternoon drifts exhibit strong longitude variations with largest values in the 210°–360° and smallest in 180°–210° sector at all seasons. The eastward drifts are largest in the premidnight and in the 240°–300° sector; the postmidnight drifts generally decrease with local time and reverse to westward close to dawn.

[11] Figure 2 shows the local time and seasonal dependence of the average zonal drifts in eight longitudinal sectors. The standard deviations are about 20 m/s during the day and 40 m/s at night, and the corresponding standard errors of the means are about 2 and 3 m/s, respectively. The large standard deviations reflect mostly the large quiet-time variability of equatorial plasma drifts during low solar flux conditions [e.g., *Fejer and Scherliess*, 2001]. The early morning drifts are strongly westward for about 1 h, especially during equinox when they have peak values of up to about 60 m/s. These equinoctial peaks are smallest at longitudes of about 240°, where the magnetic declinations have their largest values. In this sector, June solstice drifts exhibit late night eastward drift enhancements. The midday drifts have large longitude dependence with values between about 40 and 70 m/s close to noon. The evening reversal time occurs at about 1700 LT and is nearly longitude-independent during equinox. The nighttime eastward drifts are largest in the premidnight sector with peak values of about 110 m/s in the 240°–300° sector. Figure 1 shows that these peak values occur earliest and latest during June solstice and December solstice, respectively. The morning drifts reverse to westward at about 0500 LT and display their strongest seasonal variation at longitudes of about 240°.

[12] The longitudinal variations of the midday and afternoon zonal drifts are presented in Figure 3. The midday average drifts have values between about −40 to −70 m/s (corresponding to westward flow) with minima in the American sector; the afternoon averages vary from −30 to 20 m/s. In the Eastern Hemisphere, the midday and afternoon drifts have similar longitudinal dependence at all seasons, and the magnitudes of the June solstice and

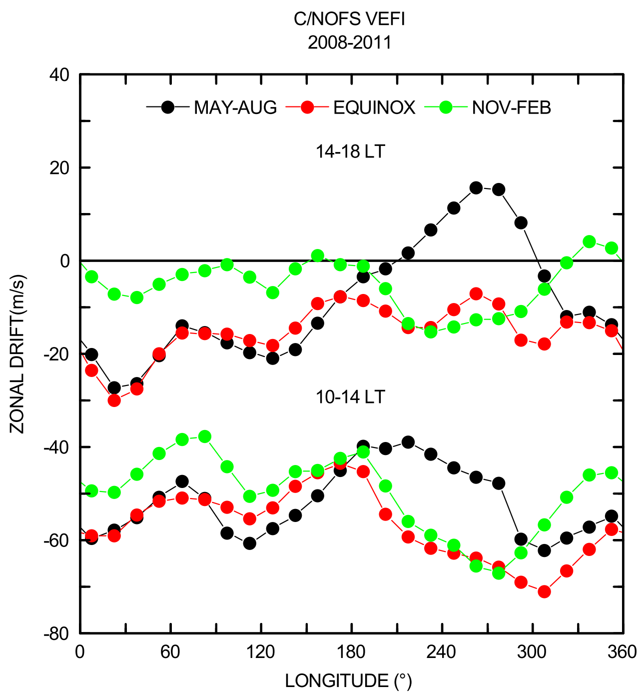

Figure 3. Average midday and afternoon average zonal drifts (positive eastward) as a function of season and longitude.

equinoctial drifts are nearly identical and considerably larger than the December solstice drifts. In the Western Hemisphere, however, the December and June solstice drifts are anticorrelated, and the equinoctial drift patterns follow those of the December solstice drifts in the 180°–300° sector and those of the June solstice drifts in the 300°–360° sector. The drift reversal from westward to eastward occurs earliest during the June solstice and in the 210°–300° sector. The afternoon equinoctial drifts exhibit a wave-4 structure with westward peaks at longitudes of about 30°, 120°, 220°, and 300°. As discussed later, this wave-4 structure is observed up to the late night period.

[13] Figure 4 illustrates the longitudinal variation of the zonal drifts in the dusk and early night sectors. Near dusk, the eastward drifts increase from the eastern to the Western Hemisphere and have very similar longitudinal dependence at all seasons. In this period, the largest peak drifts occur at longitudes of about 280° during equinox. In the 2100–2400 LT sector, the June solstice drifts are very small in the 0°–150° sector; they increase westward up to longitudes of about 280°, where they reach their largest nighttime magnitudes, and sharply decrease from 280° to 300°. The December solstice drifts do not change much with longitude and are much larger than the June solstice drifts, except at longitudes between about 210° and 300°. The equinoctial drifts again peak at longitudes of about 280° and show a clear wave-4 structure. Figures 3 and 4 suggest that the equinoctial wave-4 longitudinal structure shifts eastward in the afternoon–midnight sector.

[14] The postmidnight drifts (not shown) exhibit only weak longitudinal dependence up to about 0300 LT and have typical values of about 30 m/s. In this case, the equinoctial drifts show fairly well-developed wave-4 structure up to about 0400 LT and reverse at about 0500 LT near 300°. The June solstice drifts also reverse to westward at about 0500 LT, except in the 210°–270° sector of large positive magnetic declination, where they remain eastward up to about 0700 LT. In this sector, the late night eastward drifts are enhanced during June solstice, and the early morning equinoctial westward peaks are very weak (see Figure 2). The December solstice drift reverses to westward at about 0400 LT in the 270°–300° sector, where they have their largest westward values up to late afternoon. The June and December solstice drifts become anticorrelated in the Western Hemisphere at about 0900 LT. This anticorrelation lasts up to about the late afternoon period.

[15] Figure 5 shows bimonthly averaged zonal drifts during March–April, June–July, and September–October. These data highlight the consistent drift patterns during the vernal and autumnal equinoxes. The wave-4 structure is particularly clear on the autumnal equinoctial drifts, where the westward peak drifts occur at longitudes of about 20°, 110°, 220°, and 320°. The C/NOFS data (not shown) also indicates that wave-4 structure on the afternoon zonal drifts is already well developed during July and August. The nighttime eastward drifts are consistently stronger in the Western Hemisphere with peak values at longitudes of about 280°, as pointed out previously. Figure 5 also shows the regions of nighttime peak drift velocities shift about 20° eastward in longitude between 2000 and 0200 LT.

3.2. Comparison Results From Other Studies

[16] Figure 6 compares the average *F* region zonal drifts measured by the Jicamarca incoherent scatter radar during

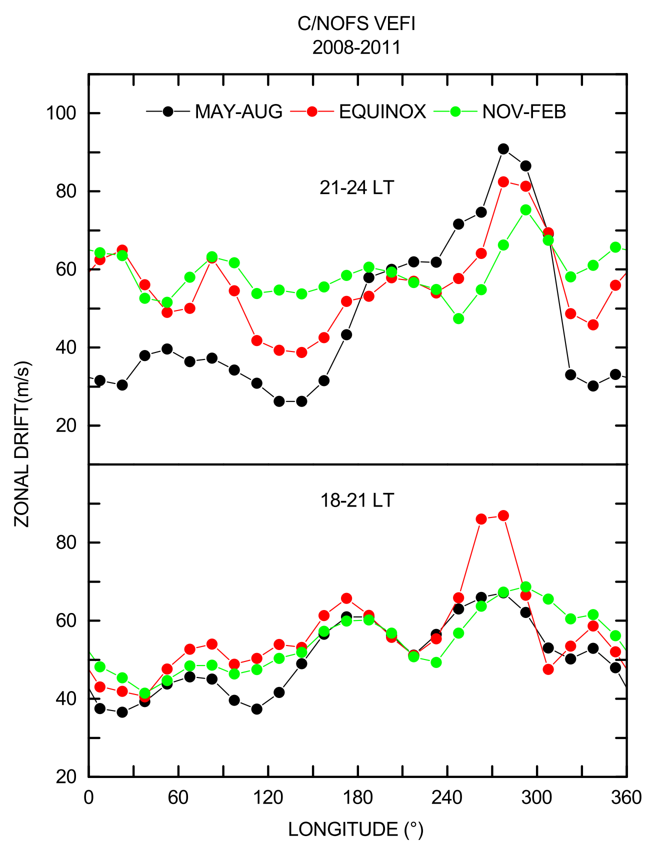

Figure 4. Average premidnight zonal drifts as a function of season and longitude.

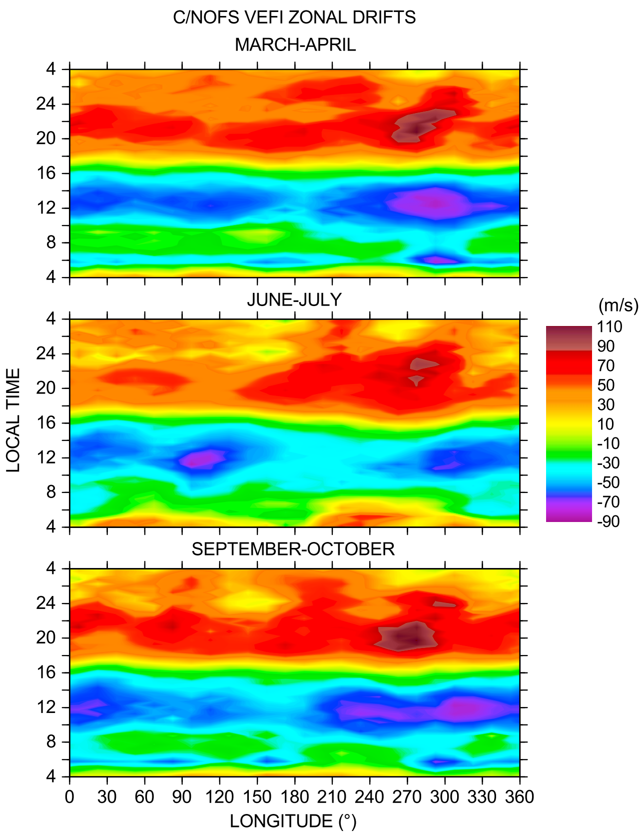

Figure 5. Bimonthly averaged zonal drifts as a function of local time and longitude.

2008–2011 and the average drifts measured by C/NOFS over a 15° longitudinal range centered over the radar site. The radar data, which correspond to averages over the 200–600 km altitudinal range, were obtained from about 30 days of measurements for each season. We note, however, that the small postmidnight plasma densities and signal-to-noise ratios during this very low solar flux period restricted most of our late night radar drifts to altitudes below about 400 km. The typical standard deviations are about 15 and 40 m/s for the daytime and nighttime radar drifts and about 20 and 45 m/s for the satellite drifts. As mentioned earlier, the standard deviations are partly due to the large quiet-time spatial and temporal variability of low solar flux equatorial drifts. Figure 6 shows generally good agreement between the radar and satellite measurements considering their accuracy, different altitudinal ranges, and especially the large longitudinal variation of the satellite drifts in the western American longitudinal sector.

[17] Quiet-time zonal drifts are driven by zonal and meridional thermospheric winds. The meridional wind results from the interhemispheric transport and are directed from summer to winter. The zonal winds are westward during the day and become eastward at about 1700 LT. The nighttime zonal drifts are a proxy for the zonal winds [e.g., *Heelis*, 2004]. Therefore, we have also examined the relationship between seasonally averaged nighttime equatorial zonal winds derived from Fabry–Perot interferometer measurements of 630.0 nm spectral emissions in northeastern Brazil (6.9°S, 38.6°W) during September 2009 to October 2010 presented by *Meriwether et al.* [2011] and our corresponding climatological drifts. These winds are eastward with average magnitudes that increase from about 40 m/s after sunset to peak values of about 90 m/s at 2100 LT and then decrease to postmidnight values of 20–30 m/s. The neutral wind and C/NOFS zonal drift local time patterns follow each other closely during December solstice and equinox, except for the larger magnitudes (by about 20 m/s) of the zonal winds before about 2300 LT. On the other hand, after about 2000 LT, the magnitudes of the June solstice C/NOFS zonal drifts are significantly smaller than the Fabry–Perot-derived neutral winds. This is particularly the case close to 2300 LT when the nighttime eastward drifts reach values as low as about 20 m/s (about 50 m/s smaller than the magnitudes of the zonal winds). These very small drift velocities are consistent with the maximum occurrence of plasma bubble drift velocity reversals from eastward to westward near midnight observed over Brazil during July–September [*Sobral et al.*, 2011].

[18] *Huang et al.* [2010] studied the longitudinal dependence of zonal ion drifts in the equatorial topside ionosphere using DMSP F13 and F14 satellite measurements at about 1800 LT during 2007–2008. In this study, the drift velocities were determined at a specific UT (longitude) relative to the minimum global equatorial daily value. These data show evening zonal drifts and plasma density with wave-4, wave-3, and wave-2 patterns during equinox, northern summer, and northern winter, respectively. Equinoctial eastward velocity peaks were observed at 30°, 120°, 210°, and 300°, respectively. Figures 3 and 4 showed that the afternoon and early night zonal C/NOFS drifts also exhibit a wave-4 structure during equinox and large eastward and westward variations in the region of large magnetic declination during June and December solstice. However, the C/NOFS data

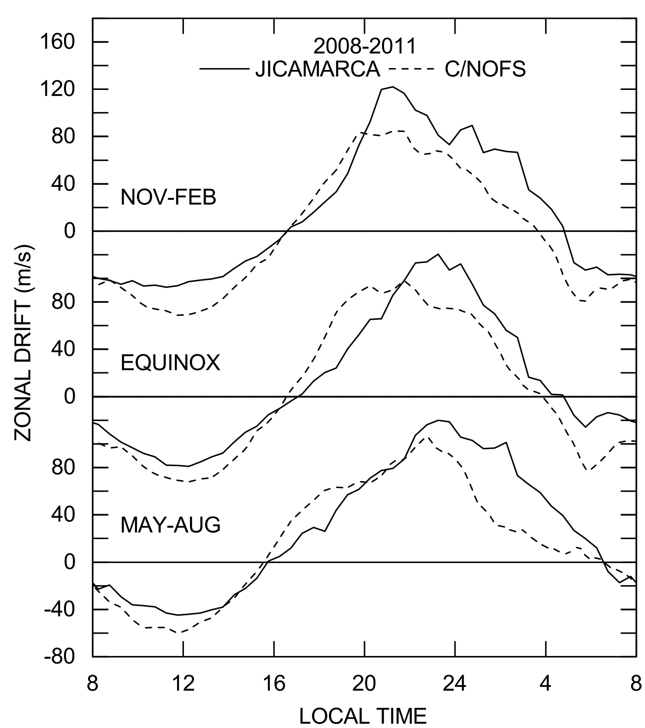

Figure 6. Comparison of average zonal drifts measured by the C/NOFS satellite over Jicamarca and the radar-measured *F* region drifts.

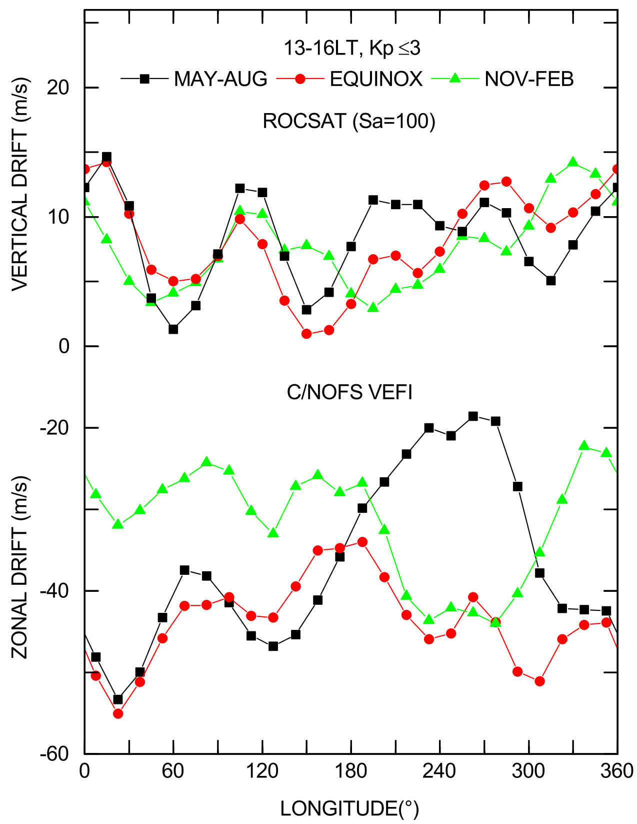

Figure 7. Seasonal and longitudinal dependence of average afternoon vertical drifts (positive upward) from ROCSAT-1 and zonal drifts (positive eastward) from C/NOFS.

show zonal drift minima at longitudes of about 30°, 120°, 210°, and 300°, whereas the higher altitude 2008 DMSP reported results show maxima at these longitudes. These different results could be due to longitudinal shifts of the wave-4 pattern with altitude and/or solar flux. *Huang et al.* [2010] suggested that meridional wind effects could explain the anticorrelated June and December solstice drifts in regions of large magnetic declination. In these regions, June solstice southward winds increase the eastward drifts in regions of negative declination and decrease in regions of positive declination; the reverse is the case during December solstice. These winds are also the most likely sources of the largely different longitudinal dependence observed in the C/NOFS Western Hemisphere June and December solstice drifts.

[19] ROCSAT-1 measurements at an altitude of about 600 km showed well-developed wave-4 longitudinal on the vertical drift velocity during late morning and early afternoon equinoctial periods [*Kil et al.*, 2008; *Fejer et al.*, 2008]. These measurements also indicate coincident peaks in the longitudinal patterns of the plasma density and upward drift velocity [*Kil et al.*, 2008]. Figure 7 presents the longitudinal variations of the quiet-time early afternoon equinoctial C/NOFS zonal drifts and of the low solar flux ($Sa = 100$) vertical model drifts derived by *Fejer et al.* [2008] from ROCSAT-1 data. Figure 7 indicates that early afternoon zonal and vertical plasma drifts have similar longitudinal dependence in the Eastern Hemisphere and anticorrelated longitudinal variations during June and December solstice in the Western Hemisphere. These results highlight the importance of magnetic declination effects on the low-latitude plasma drifts.

[20] Recently, *Huang et al.* [2012] showed that plasma density and drift velocities from C/NOFS and neutral densities from GRACE during the 2008–2010 deep solar minimum all display wave-4 structures with climatology similar to that of DE-3 nonmigrating tides [e.g., *Hagan and Forbes*, 2002, 2003]. In this study, average equatorial zonal drifts during the 2008, 2009, and 2010 June solstice were derived from the VEFI meridional electric fields projected to the magnetic equator using the International Reference Geomagnetic Field model. These drifts are consistent with our results, even though they correspond to a broader (longitude-dependent) range of apex heights (magnetic latitudes) than used in our study. *Huang et al.* [2012] showed that nightside June solstice VEFI zonal drifts evolve from early to late local times with an eastward phase change which is most noticeable from about 180° to 360° longitude. We have seen in Figure 5 that this phase shift is most pronounced at longitudes of about 270°, where the premidnight eastward drifts are largest. *Huang et al.* [2012] also pointed out that broad plasma decreases observed most often in the 300°–360° longitudinal range by C/NOFS, and previously on CHAMP and DMSP data [e.g., *Huang et al.*, 2009, 2011], are colocated with regions of large downward drifts and minima in the zonal drifts and are related to deep minima in the plasma density tidal patterns.

[21] The longitudinal variation of the low-latitude plasma drifts is determined mostly by the effects of migrating and nonmigrating lower atmospheric tides and *E* and *F* region neutral winds and are also affected by geomagnetic field and solar-cycle-dependent conductivities. The effects of various ionospheric parameters on the low-latitude vertical drifts were discussed in various experimental [e.g., *West and Heelis*, 1996; *Hartman and Heelis*, 2007] and modeling [e.g., *Eccles*, 1998; *Fang et al.*, 2009; *Maute et al.*, 2012] studies. The recent study of *Maute et al.* [2012], in particular, examined in detail the relative roles of nonmigrating tides and height-dependent winds on the equinoctial equatorial vertical drifts. So far, detailed numerical studies have not been carried out on the longitudinal dependence of low-latitude zonal plasma drifts. These modeling studies would provide more detailed information on the electrodynamic effects of various lower atmospheric and ionospheric processes and parameters.

4. Summary

[22] We have shown that the equatorial zonal plasma drifts measured by C/NOFS are westward from about sunrise to late afternoon, with peak magnitudes between about 40 and 70 m/s close to noon and vary significantly with season and longitude. The early morning equinoctial drifts have large short-lived peaks over a large range of longitudes. The midday and afternoon daytime drifts have much larger longitudinal and seasonal dependence in the Western than in the Eastern Hemisphere. The midday and afternoon June and December solstice drifts are anticorrelated in regions of large magnetic declination. The equinoctial drifts exhibit wave-4 structures in the afternoon–late night period. The evening reversal time also changes with season and longitude with largest variations in the Western Hemisphere. The nighttime

eastward drifts have peak magnitudes between about 50 and 100 m/s, with largest values in the premidnight sector and at longitudes near 270° at all seasons. The postmidnight drifts generally decrease with increasing local time. The C/NOFS zonal drifts are in good agreement with the incoherent scatter radar-measured drifts.

[23] **Acknowledgments.** This work was supported by the Aeronomy Program, Division of Atmospheric Sciences of the National Science Foundation through grant AGS-1068104 and by NASA through grants NNH12C02C and NNX09ANSSG. The Jicamarca Radio Observatory is a facility of the Instituto Geofisico del Peru and is operated with support from the NSF cooperative agreement AGS-0905448 through Cornell University.

[24] Robert Lysak thanks the reviewers for their assistance in evaluating this paper.

References

Bhattacharyya, A., S. Basu, K. M. Groves, C. E. Valladares, and R. Sheehan (2001), Dynamics of equatorial F region irregularities from spaced receiver scintillation observations, *Geophys. Res. Lett.*, *28*(1), 119–122.

Chapagain, N. P., M. J. Taylor, and J. V. Eccles (2011), Airglow observations and modeling of *F* region depletion zonal velocities over Christmas Island, *J. Geophys. Res.*, *116*, A02301, doi:10.1029/2010JA015958.

Chapagain, N. P., J. J. Makela, J. W. Meriwether, D. J. Fisher, R. A. Buriti, and A. F. Medeiros (2012), Comparison of nighttime zonal neutral winds and equatorial plasma bubble drift velocities over Brazil, *J. Geophys. Res.*, *116*, A02301, doi:10.1029/2012JA017620.

Coley, W. R., and R. A. Heelis (1989), Low-latitude zonal and vertical ion drifts seen by DE-2, 1989, *J. Geophys. Res.*, *94*(A6), 6751–6761, doi:10.1029/JA004iA06p06751.

Coley, W. R., R. A. Heelis, and N. W. Spencer (1994), Comparison of low-latitude ion and neutral zonal drifts using DE-2 data, *J. Geophys. Res.*, *99*(A1), 341–348, doi:10.1029/93JA02205.

Dao, E., M. C. Kelley, P. Roddy, J. Retterer, O. de La Beaujardiere, and Y.-J. Su (2011), Longitudinal and seasonal dependence of nighttime equatorial plasma density irregularities during solar minimum detected on the C/NOFS satellite, *Geophys. Res. Let.*, *38*, L10104, doi:10.1029/2011GL47046.

de la Beaujardiere, O., et al. (2004), C/NOFS: A mission to forecast scintillations, *J. Atmos. Sol. Terr. Phys.*, *66*, 1573–1591, doi:10.1016/j.jastp.2004.07.030.

Eccles, J. V. (1998), A simple model of low-latitude electric fields, *J. Geophys. Res.*, *103*(A11), 26,699–26,708.

Fang, T.-W., H. Kil, G. Milward, A. D. Richmond, J.-Y. Liu, and S.-J. Oh (2009), Casual link of the wave-4 structures in plasma density and vertical drift in the low-latitude ionosphere, *J. Geophys. Res.*, *114*, A10315, doi:10.1029/2009JA014460.

Fejer, B. G. (1997), Electrodynamics of the low latitude ionosphere: Recent results and future challenges, *J. Atmos Sol. Terr. Phys.*, *59*, 1456–1482, doi:10.1016/s1364-6826(96)00 149–6.

Fejer, B. G. (2011), Low latitude ionospheric electrodynamics, *Space Sci. Rev.*, *158*(1), 145–166, doi:10.1007/s11214-010-9690-7.

Fejer, B. G., and L. Scherliess (2001), On the variability of equatorial *F* region vertical plasma drifts, *J. Atmos. Sol. Terr. Phys.*, *63*, 893–897.

Fejer, B. G., E. R. de Paula, S. A. Gonzales, and R. F. Woodman (1991), Average vertical and zonal *F* region plasma drifts over Jicamarca, *J. Geophys. Res.*, *96*(A8), 13,901–13,906, doi:10.1029/91JA01171.

Fejer, B. G., J. R. Souza, A. S. Santos, and A. E. Costa Pereira (2005), Climatology of *F* region zonal plasma drifts over Jicamarca, *J. Geophys. Res.*, *110*, A12310, doi:10.1029/2005JA011324.

Fejer, B. G., J. W. Jensen, and S.-Y. Su (2008), Quiet time equatorial *F* region vertical plasma drift model derived from ROCSAT-1 observations, *J. Geophys. Res.*, *113*, A05354, doi:10.1029/2007JA012801.

Hagan, M. E., and J. M. Forbes (2002), Migrating and non-migrating diurnal tides in the middle and upper atmosphere excited by tropospheric latent heat release, *J. Geophys. Res.*, *107*(D24), 4754, doi:10.1029/2001JD001236.

Hagan, M. E., and J. M. Forbes (2003), Migrating and non-migrating semidiurnal tides in the middle and upper atmosphere excited by tropospheric latent heat release, *J. Geophys. Res.*, *108*(A2), 1064, doi:10.1029/2002JA009466.

Hartman, W. A., and R. A. Heelis (2007), Longitudinal variations in the equatorial vertical drift in the topside ionosphere, *J. Geophys. Res.*, *112*, A03305, doi:10.1029/2006JA011773.

Heelis, R. A. (2004), Electrodynamics in the low and middle latitude ionosphere: A tutorial, *J. Atmos. Sol. Terr. Phys.*, *66*(10), 825–838, doi:10.1016/j.jastp.2004.01.034.

Huang, C. Y., F. A. Marcos, P. A. Roddy, M. R. Hairston, W. R. Coley, C. Roth, S. Bruinsma, and D. E. Hunton (2009), Broad plasma decreases in the equatorial ionosphere, *Geophys. Res. Lett.*, *36*, L00C04, doi:10.1029/2009GL039423.

Huang, C.-S., F. J. Rich, O. de La Beaujardiere, and R. A. Heelis (2010), Longitudinal and seasonal variations of the equatorial ionospheric ion density and eastward drift velocity in the dusk sector, *J. Geophys. Res.*, *115*, A02305, doi:10.1029/2009JA014503.

Huang, C. Y., S. H. Daly, P. A. Roddy, and E. K. Sutton (2011), Periodic structures in the equatorial ionosphere, *Radio Sci.*, *46*, RD0D14, doi:10.1029/2010RS004569.

Huang, C. Y., P. A. Roddy, E. K. Sutton, R. Stoneback, R. F. Pfaff, L. C. Gentile, and S. H. Delay (2012), Ion-neutral coupling during deep solar minimum, *J. Atmos. Sol. Terr. Phys.*, doi:10.1016/j.jastp.2012.11.009.

Jensen, J. W., and B. G. Fejer (2007), Longitudinal dependence of middle and low latitude zonal plasma drifts measured by DE-2, *Ann. Geophys.*, *25*, 2551–2559.

Kil, H., E. R. Talaat, S.-J. Oh, L. J. Paxton, S. L. England, and S.-Y. Su (2008), Wave structures of the plasma density and vertical ExB drift in low-latitude *F* region, *J. Geophys. Res.*, *113*, A09312, doi:10.1029/2018JA013106.

Maute, A., A. D. Richmond, and R. G. Roble (2012), Sources of low-latitude ionospheric ExB drifts and their variability, *J. Geophys. Res.*, *117*, A06312, doi:10.1029/2011JA017502.

Maynard, N. C., T. L. Aggson, F. A. Herrero, M. C. Liebrecht, and J. L. Saba (1995), Average equatorial zonal and vertical ion drifts determined from San Marco DC electric field measurements, *J. Geophys. Res.*, *100*(17), 17,465–17,479, doi:10.1029/95JA00767.

Meriwether, J. W., J. J. Makela, Y. Huang, D. J. Fisher, R. A. Buriti, A. F. Medeiros, and H. Takahashi (2011), Climatology of the nighttime equatorial thermospheric winds and temperatures over Brazil near solar minimum, *J. Geophys. Res.*, *116*, A04322, doi:10.1029/2011JA016477.

Murphy, J. A., and R. A. Heelis (1986), Implication of the relationship between electromagnetic drift components at mid and low latitude, *Planet. Space Sci.*, *34*, 645–655.

Pacheco, E. E., R. A. Heelis, and S.-Y. Su (2011), Super rotation of the ionosphere and quiet time zonal ion drifts at low and middle latitudes observed by Republic of China Satellite-1 (ROCSAT-1), *J. Geophys. Res.*, *116*, A11329, doi:10.1029/2011JA016786.

Pavlov, A. V. (2006), The role of the zonal ExB drift in the low-latitude ionosphere at high solar activity near equinox from a three-dimensional numerical model, *Ann. Geophys.*, *24*, 2553–2572.

Pfaff, R., et al. (2010), Observations of DC electric fields in the low-latitude ionosphere and their variation with local time, longitude, and plasma density during extreme solar minimum, *J. Geophys. Res.*, *115*, A12324, doi:10.1029/2010JA016023.

Richmond, A. D. (1995), Ionospheric electrodynamics, in *Handbook of Atmospheric Electrodynamics*, vol. 2, edited by H. Volland, pp. 249–290, CRC Press, Boca Raton, Fla.

Sheehan, R. E., and C. E. Valladares (2004), Empirical ionospheric zonal drift model and vertical drift statistics from UHF scintillation measurements in South America, *Ann. Geophys.*, *22*, 3177–3193.

Sobral, J. H. A., et al. (2009), Ionospheric zonal velocities at conjugate points over Brazil during the COPEX campaign: Experimental observations and theoretical validations, *J. Geophys. Res.*, *114*, A04309, doi:10.1029/2008JA013896.

Sobral, J. H. A., et al. (2011), Midnight reversal of ionospheric plasma bubble eastward velocity to westward velocity during geomagnetically quiettime: Climatology and its model validation, *J. Atmos. Sol. Terr. Phys.*, *73*, 1520–1528.

Su, S.-Y., C. K. Chao, and C. H. Liu (2009), Cause of different local time distribution in the postsunset equatorial ionospheric irregularity occurrences between June and December solstices, *J. Geophys. Res.*, *114*, A04321, doi:10.1029/2008JA013858.

Valladares, C. E., R. E. Shehan, S. Basu, H. Kuenzler, and J. Espinoza (1996), The multi-instrumented studies of equatorial thermosphere aeronomy scintillation system: Climatology of zonal drifts, *J. Geophys. Res.*, *101*(A12), 26,839–26,850, doi:10.1029/96JA00183.

Wan, W., L. Liu, X. Pi, M.-L. Zhang, B. Ning, J. Xiong, and F. Ding (2008), Wavenumber-4 patterns of the total electron content over the low latitude ionosphere, *Geophys. Res. Lett.*, *35*, L12104, doi:10.1029/2008GL033755.

West, K. H., and R. A. Heelis (1996), Longitudinal variations in ion composition in the morning and evening topside equatorial ionosphere near solar minimum, *J. Geophys. Res.*, *101*(A4), 7951, doi:10.1029/95JA03380.